



UNIVERSIDAD NACIONAL DE COLOMBIA

Study of CP symmetry in B^\pm to three body decays using LHCb experiment opendata

Jonnatan Pereira Betancur

Universidad Nacional de Colombia
Faculty of Sciences, Physics department
Bogotá, Colombia
2022

Study of CP symmetry in B^\pm to three body decays using LHCb experiment opendata

Jonnatan Pereira Betancur

Work presented as partial requirement to obtain the degree of:
Physicist

Directors:

Carlos Eduardo Sandoval Usme Ph.D.

Diego Alejandro Milanes Carreno Ph.D.

Line of research:

Experimental particle physics

Research group:

FENyX - Phenomenology and experimental particles

Universidad Nacional de Colombia
Faculty of Sciences, Physics department
Bogotá, Colombia

2022

Abstract

Charmless decays of charged B mesons to three-body final states are studied for $K^+K^-\pi^\pm$, $\pi^+\pi^-\pi^\pm$ and $K^+K^-K^\pm$ systems. Particle identification and other event selection criteria are applied to LHCb opendata from 2011 at a 7 TeV center-of-mass energy and 1.0 fb^{-1} integrated luminosity. Global raw asymmetries $A_{CP}(B^\pm \rightarrow K^+K^-\pi^\pm) = -0,065 \pm 0,022 (2.899\sigma)$, $A_{CP}(B^\pm \rightarrow \pi^+\pi^-\pi^\pm) = 0,045 \pm 0,009 (5.103\sigma)$ and $A_{CP}(B^\pm \rightarrow K^+K^-K^\pm) = -0,057 \pm 0,018 (3.152\sigma)$ are calculated through Dalitz plot amplitude analysis, finding evidence and observations of direct CP violation. More data analysis strategies are developed and applied throughout the study of the systems, leading to results of even higher significance in localized regions of the phase space. The presented uncertainties are purely statistical, lower significance is expected if processes involving systematic uncertainties are considered.

Keywords: CP symmetry, pions, kaons, charged B mesons, Dalitz plot

Decaimientos de mesones B cargados a tres cuerpos sin contribuciones charm son estudiados en sistemas $K^+K^-\pi^\pm$, $\pi^+\pi^-\pi^\pm$ y $K^+K^-K^\pm$. Se aplican criterios de identificación y selección de eventos sobre datos abiertos del experimento LHCb tomados en 2011 a 7 TeV de energía de centro de masa y 1.0 fb^{-1} luminosidad integrada. Resultados crudos de asimetría $A_{CP}(B^\pm \rightarrow K^+K^-\pi^\pm) = -0,065 \pm 0,022 (2.899\sigma)$, $A_{CP}(B^\pm \rightarrow \pi^+\pi^-\pi^\pm) = 0,045 \pm 0,009 (5.103\sigma)$ y $A_{CP}(B^\pm \rightarrow K^+K^-K^\pm) = -0,057 \pm 0,018 (3.152\sigma)$ son calculados a través del análisis de amplitud en graficos de Dalitz, encontrando evidencia y observación de violación CP directa. Mas estrategias de análisis de datos son desarrolladas y aplicadas durante el estudio de los sistemas, llevando a resultados de aún mayor significancia en regiones específicas del espacio de fase. Las incertidumbres presentadas son puramente estadísticas, significancias menores se esperan en caso de considerar procesos que involucren incertidumbres sistemáticas.

Palabras clave: Simetría CP , piones, kaones, mesones B cargados, gráficos de Dalitz

Contents

Abstract	v
1. Introduction	2
2. Theoretical framework	3
2.1. P , T and C symmetries	3
2.2. CKM Matrix	3
2.3. CP Violation	4
3. Data analysis	7
3.1. Dataset parameters	7
3.2. Particle identification and selection criteria	8
3.3. Asymmetry, statistical uncertainty and significance	10
4. Results	11
4.1. Signal cleansing	11
4.2. Adaptive binning of the Dalitz plots	14
4.3. Study of the asymmetry	15
4.3.1. $B^\pm \rightarrow K^+ K^- \pi^\pm$	16
4.3.2. $B^\pm \rightarrow \pi^+ \pi^- \pi^\pm$	17
4.3.3. $B^\pm \rightarrow K^+ K^- K^\pm$	18
5. Conclusions	19
A. Attachment: Table of particles	20
Bibliography	21

1. Introduction

In 1957, Chien-Shiung Wu discovered the violation of the parity (P) symmetry through an experiment involving β decays in cobalt-60 nuclei. It was the first report of phenomena breaking the P symmetry, and it was a process governed by weak interactions specifically. After some theoretical work made by Lev Landau, and by Lee and Yang, the incorporation of the charge (C) symmetry along with parity i.e. a CP operator seemed to resolve the situation. Only a few years later in 1964, Jim Cronin presented results of CP violation in neutral kaon decays to two pions [1]. Theoretical efforts were made, passing through a successful model called superweak. In 1973, Makoto Kobayashi and Toshihide Maskawa generalized the work made by Nicola Cabibbo and produced the first theory of CP violation in the context of the Standard Model [2].

Theoretically, the CP violation consists on the fundamental fact that said symmetry breaks in any theory with complex coupling constants in the Lagrangian, that cannot be eluded by phase redefinitions of the fields [3]. These constants are present in the Cabibbo-Kobayashi-Maskawa (CKM) matrix, which explains the weak interactions between quarks.

Three different systems of charged B meson decays to three body final states will be studied in the present work. The CP violation (CPV) mechanism leading to the observables in such systems is *direct* CPV , which would explain the interference patterns or resonances between the amplitudes of intermediate quasi-two-body states that are present in the phase space [4]. The data analysis technique to be used is the Dalitz plot, which is a 2-D visualization of the phase space in decays of one to three bodies, providing information about the dynamics of the physical system through different combinations of the two-body invariant masses representing the intermediate states [5].

Being able to account for differences in the number of events coming from mesons B^+ with respect to B^- after an appropriate selection and particle identification criteria in experimental data, will lead to evidence and observations that the studied physical systems exhibit CPV based on the significance of the results.

2. Theoretical framework

2.1. P, T and C symmetries

The following are operations of potential symmetries in the Lagrangian of a field theory

Parity P	$(t, \vec{x}) \rightarrow (t, -\vec{x})$
Time reversal T	$(t, \vec{x}) \rightarrow (-t, \vec{x})$
Charge conjugation C	Particle \rightarrow Anti-particle

Combining the charge and parity operators, i.e. having the CP operator, ends up replacing the particle by its antiparticle and reversing momentum and helicity in a system. For example, a left-handed electron e_L^- is transformed into a right-handed positron e_R^+ under CP . Electromagnetic, gravitational and strong interactions are invariant under C , P and CP transformations [6]. Some of the systems involving weak interactions that break CP symmetry are studied in the present work.

Until now, no physical systems have been found to break CPT symmetry, making it a so called *exact symmetry*. Its conservation is necessary in any local Lagrangian field theory [3] such as special relativity and quantum field theory.

2.2. CKM Matrix

The Cabbibo-Kobayashi-Maskawa (CKM) matrix $V_{CKM} = V$ is a unitary $VV^\dagger = 1$ matrix that describes the weak interactions of quarks. The following expression relates the weak eigenstates (d', s', b') and mass eigenstates (d, s, b)

$$\begin{bmatrix} d' \\ s' \\ b' \end{bmatrix} = \begin{bmatrix} V_{ud} & V_{us} & V_{ub} \\ V_{cd} & V_{cs} & V_{cb} \\ V_{td} & V_{ts} & V_{tb} \end{bmatrix} \begin{bmatrix} d \\ s \\ b \end{bmatrix} \quad (2-1)$$

V is the 3×3 matrix and its elements define the strength of the interactions between a given pair of quarks [7].

There's many different ways to express the matrix elements in terms of three rotation angles and one phase, all equally functional in a theoretical perspective but some are more practical for phenomenological purposes [8].

The *Wolfenstein parametrization* is commonly used [6]

$$V = \begin{bmatrix} 1 - \lambda^2/2 & \lambda & A\lambda^3(\rho - i\eta) \\ -\lambda & 1 - \lambda^2/2 & A\lambda^2 \\ A\lambda^3(1 - \rho - i\eta) & -A\lambda^2 & 1 \end{bmatrix} \quad (2-2)$$

plus terms of higher order in lambda ($+\mathcal{O}(\lambda^4)$). Elements V_{13} and V_{31} , containing an imaginary part, are the ones that naturally change in the complex conjugate form of the amplitude. More information involving these relevant elements of the CKM matrix will be presented in the next section.

2.3. CP Violation

The **CPV in decay**, also called *direct CPV*, consists on the implications of the fact that the decay amplitude of the particle going to a final state f is different than that of its anti-particle going to \bar{f} . It is present in both charged and neutral systems.

The **CPV in mixing**, also called *indirect CPV*, has to do with the mass eigenstates in neutral kaon systems being different than the *CP* eigenstates.

The **CPV through the interference between a decay amplitude and mixing**, sometimes occurs as a combination of the other two and takes place commonly in neutral B meson decays. [3].

More on the CPV in decay

The decay amplitudes of particle and anti-particle, specifically for charged B mesons, can be defined as

$$A_f = \langle f | H | B^+ \rangle = \sum_i A_i e^{i(\delta_i + \phi_i)}$$

$$\bar{A}_{\bar{f}} = \langle \bar{f} | H | B^- \rangle = e^{2i(\xi_f - \xi_B)} \sum_i A_i e^{i(\delta_i - \phi_i)}$$

where ξ_f comes out of the transformation

$$CP |B^+\rangle = e^{2i\xi_B} |B^-\rangle$$

and ξ_f also comes from a transformation law between a final state f and its CP conjugate. Phase freedom exists for both ξ_B and ξ_f such that they can be rather arbitrary, due to quark flavor symmetries in strong interactions [3]. The following expression can be obtained from the defined decay amplitudes

$$\left| \frac{\bar{A}_{\bar{f}}}{A_f} \right| = \left| \frac{\sum_i A_i e^{i(\delta_i - \phi_i)}}{\sum_i A_i e^{i(\delta_i + \phi_i)}} \right| \quad (2-3)$$

Conservation of CP implies that all weak phases ϕ_i are the same, then $|\bar{A}_{\bar{f}}/A_f| \neq 1$ leads to the symmetry breaking inevitably. Another implication of the decay amplitudes can be observed in the following expression

$$|\bar{A}|^2 - |A|^2 = 2 \sum_{i,j} A_i A_j \sin(\phi_i - \phi_j) \sin(\delta_i - \delta_j) \quad (2-4)$$

In order to find a difference in the decay amplitudes, at least two weak phase terms must be different, as well as their associated strong phase terms

$$\phi_i \neq \phi_j; \quad \delta_i \neq \delta_j$$

Also the other way around, finding a difference in the decay amplitudes implies that elements i and j lead to different strong and weak phases. This is very important because the decay amplitudes are the quantities directly related to the physical observables.

Feynman diagrams of two different decay mechanisms are presented for the $B^- \rightarrow K^+ K^- \pi^-$ system. The Tree-level mechanism is associated to the $V_{13} = V_{ub}$ element of the CKM matrix 2-1, accounting for a quark flavor transition ($b \rightarrow u$)

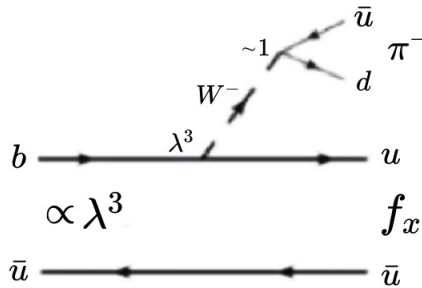


Figure 2-1.: Tree-level diagram for the $B^- \rightarrow K^+ K^- \pi^-$ decay

while the Penguin mechanism is associated to the $V_{31} = V_{td}$ element of the CKM matrix, accounting for a quark flavor transition ($b \rightarrow (u, c, t) \rightarrow d$)

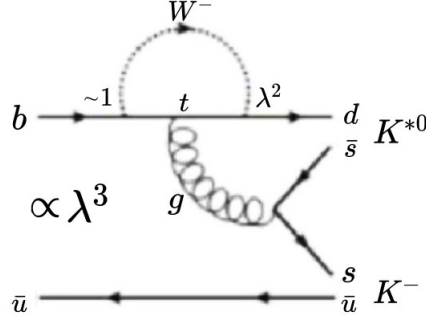


Figure 2-2.: Penguin diagram for the $B^- \rightarrow K^+ K^- \pi^-$ decay

Intermediate states such as the ones presented above, f_x and K^{*0} , would necessarily be neutral in systems with three charged mesons as final states, since there is no meson with charge ± 2 , i.e. there could be no possible quark-antiquark combination such that their net charge is equal to ± 2 . There exist, of course, other three-body final state configurations having for example a charged intermediate state and a neutral bachelor hadron, such that a ± 1 net charge is given.

Asymmetries in charged B meson decays are from direct CP violation. In terms of the decay width, the asymmetry is defined as

$$\mathcal{A}_f = \frac{\Gamma(B^- \rightarrow \bar{f}) - \Gamma(B^+ \rightarrow f)}{\Gamma(B^- \rightarrow \bar{f}) + \Gamma(B^+ \rightarrow f)} \quad (2-5)$$

and more directly practical for experimental results, in terms of the decay amplitudes [3] as

$$\mathcal{A}_f = \frac{|\bar{A}|^2 - |A|^2}{|\bar{A}|^2 + |A|^2} \quad (2-6)$$

3. Data analysis

The work presented here is based on opendata from the first run of the LHC. Specifically, the data were collected out of pp collisions by the LHCb detector at a 7 TeV center-of-mass energy and 1.0 fb^{-1} integrated luminosity in 2011 [9].

The dataset contains exactly 8'556.118 events from both up and down directions of the magnetic field in the detector. It is treated as a whole with no distinction in the analysis, ignoring the contribution that this fact could give to the systematic uncertainties involving the possible differences in the efficiency of the magnets polarity. Actually, only statistical uncertainties are considered. All the events correspond to three-body final state systems.

3.1. Dataset parameters

Events in the dataset contain the following information for each of the three final state particles:

- Cartesian components of the momentum (P_x, P_y, P_z)
- Charge, taking ± 1 values
- Likelihood or probability of being a kaon or a pion, from 0 to 1
- Boolean value determining whether it is a muon
- Statistical test χ_{IP}^2 value associated to the track impact parameter

χ_{IP}^2 is defined by projecting the trajectory of the particle in question back to the collision vertex. B^\pm candidates must come from the collision vertex, while the three final state tracks must not. There is no χ_{IP}^2 for the B^\pm candidates in the dataset.

Aside from the parameter triples defining attributes to the final state particles separately, there are two additional parameters that correspond to the event. One is associated to the initial state of the decay, while the other is a direct connection between the initial and the final state.

There is the Flight Distance of each event, which is the trajectory of the B^\pm meson candidates from the collision point to their decay point and is associated to their mean lifetime. Said lifetime is about $1,6 \times 10^{-12}$ s, therefore the Flight Distance is low but not null.

There is also a χ^2 for each event, which associates the B^\pm meson decay vertex and the tracks of the three final state particles. Lower values of this parameter indicate that the tracks are more likely to have been originated in a common point.

3.2. Particle identification and selection criteria

First of all, the three final state particles are set not to be muons, then they must meet the requirements of being a certain combination of hadrons on each decay system as follows:

- In $KK\pi$, the probability used to filter the desired hadrons is set to be higher than 0.75, while the probability to filter the non-desired hadrons is set to be lower than 0.45.
- In $\pi\pi\pi$, the probabilities used to filter the desired and non-desired hadrons are set to be higher than 0.75 and lower than 0.25 respectively.
- In KKK , the probabilities used to filter the desired and non-desired hadrons are set to be higher than 0.7 and lower than 0.3 respectively.

Naturally, the net charge of the final state three-hadron systems must be ± 1 , just as well as the charge of the B mesons from the initial state in order to fulfill charge conservation. This condition is met by all events in the dataset.

Four-vectors of the final state particles are composed by the three cartesian momentum components from the dataset and the literature mass of the particle in question. Then it is possible to obtain m_B , the invariant mass reconstructed from the three four-vectors which is the resulting quantity to represent the B^\pm meson candidate on each event.

Beyond having a combination of hadrons that effectively represents the charged B candidates, the objects of interest for the Dalitz plot analysis are the squared two-body invariant masses ($m_{\pi^+\pi^-}^2, m_{K^\pm\pi^\mp}^2, m_{K^+K^-}^2$) of neutral intermediate states R^0 . Said intermediate state is illustrated in Figure **3-1**

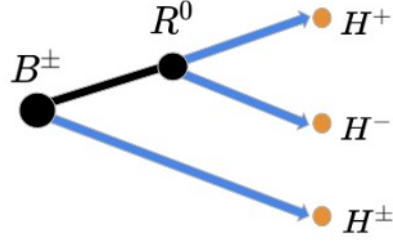


Figure 3-1.: Schematic representation of a $B^\pm \rightarrow H^+ H^- H^\pm$ decay, passing through a R^0 neutral intermediate state

The objects of interest for the Dalitz plot analysis are, more specifically for each system

- $m_{K^+K^-}^2$ and $m_{K^\pm\pi^\mp}^2$ in $KK\pi$
- $m_{\pi^+\pi^-}^2$ and $m_{\pi^+\pi^-}^2$ in $\pi\pi\pi$
- $m_{K^+K^-}^2$ and $m_{K^+K^-}^2$ in KKK

where the *high* and *low* objects refer to a symmetrization of the Dalitz plots in the $\pi\pi\pi$ and KKK systems, consisting simply in organizing the pair of $m_{H^+H^-}^2$ hadronic objects on each event such that $m_{H^+H^-}^2 < m_{H^+H^-}^2$.

Selection criteria related to the kinematics is the same for all three systems, except for the window of the reconstructed mass m_B around its value in the literature $m_{PDG}(B)$, which is selected to be slightly different in the $KK\pi$ system

- Flight Distance > 3 mm
- $\chi^2 < 12$
- $\chi_{IP}^2 > 16$ (for at least 1 track)
- $P_T > 1700$ MeV
- $|m_R - m_D| > 30$ MeV
- $|m_B - m_{PDG}(B)| < m_{window}$

where

$$m_{window} = \begin{cases} 45 \text{ MeV, for } K^+K^-\pi^\pm \\ 40 \text{ MeV, for } \pi^+\pi^-\pi^\pm \text{ and } K^+K^-K^\pm \end{cases} \quad (3-1)$$

Variables m_D and m_R refer to the D^0 meson and resonant intermediate state R^0 masses respectively. The selection criterion involving these is what removes charm contributions in the decay channels.

3.3. Asymmetry, statistical uncertainty and significance

The observable quantity coming from the direct CPV formalism, i.e. what is experimentally measured, is the squared decay amplitude $|A|^2 = N(B \rightarrow f)$. The left side of the expression already appeared in equation 2-6, and then N refers to the number of events of a given final state, which results from the data selection. The simple asymmetry expression to be used for computation purposes would be

$$\mathcal{A} = \frac{N^- - N^+}{N^- + N^+} \quad (3-2)$$

The count of final states to calculate asymmetry with in the present work, are the reconstructed two-body objects coming from the charged B decays, where the sign is naturally given by the sum of the charges of the three final state hadrons. More specifically, N^+ is the number of neutral intermediate states $m_{\pi^+\pi^-}$, $m_{K^\pm\pi^\mp}$ or $m_{K^+K^-}$ coming from a final state of +1 net charge, and N^- is the same for final states of -1 net charge.

While the definition of \mathcal{A} is the base of the asymmetry measurement, and has been referred to as *asymmetry* in the present work, this expression that only considers event counts is actually a *raw asymmetry* $\mathcal{A} = A_{raw}$ from an experimental perspective, and it is important to understand that it is only the first approximation to a formal result. More will be discussed in the chapter of Results.

With the asymmetry 3-2 it is then possible to calculate the statistical uncertainty using the following formula

$$\sigma_{\mathcal{A}} = \sqrt{\frac{1 - \mathcal{A}^2}{N^- + N^+}} \quad (3-3)$$

and finally the **significance** of the results would be the asymmetry value divided by its statistical uncertainty, and is presented in sigma units (σ). In particle physics a result over 3 sigma is called “evidence”, while one with 5 or more sigma is called “observation” [9].

4. Results

The computational work was made through the open-source data analysis framework ROOT.

4.1. Signal cleansing

Filtering the data with appropriate particle identification and selection criteria leads to the events that are well suited to represent the charged B mesons from the initial state. The filtering process to obtain these initial state candidates is also called “cutting” process, where each cut is a single item of the kinematic selection or particle identification.

In a dataset, the **signal** events are those that correspond directly to the physical system of interest, while the **background** events are everything else collected during the detection process. The set of events passing through the cuts contain the signal, while the discarded events are part of the background. It is possible to reconstruct the invariant mass of the initial state using the entirety of the events in the dataset, before applying any cuts, simply by treating all the final state particles tentatively as the specific hadrons of the systems that are studied, i.e. using the literature masses of the desired mesons and the dataset momentum variables to fill the four-vectors regardless of any selection items.

Figure 4-1 shows histograms corresponding to the reconstructed masses of the initial state before any cuts on the left, and filtered ones after cuts on the right. The only cut that is not applied to the filtered histograms is the one corresponding to the mass window around the charged B value from the literature, however, the mass window is shown as the region inside dotted lines on all plots. Considering that the entire dataset contains over 8.5 million events, where roughly about 1 million of each final state particles are muons, and $m_{PDG}(B) = 5279,25 \pm 0,17$ MeV directly taken from the Particle Data Group archives [10], the following observations can be made about the histograms presented:

- $\pi\pi\pi$ plot with no cuts 4.1(a) has a single prominent and wide peak at around 5230 MeV, the signal of interest would be within it, to the right. The corresponding filtered plot 4.1(b) contains 175575 events, where 13091 of them are within the mass window.
- KKK plot with no cuts 4.1(c) has a small peak around $m_{PDG}(B)$ and an important one at around 5420 MeV. The signal of interest would be within the small peak. The

corresponding filtered plot 4.1(d) contains 7851 events, where 5954 of them are within the mass window.

- $KK\pi$ plot with no cuts 4.1(e) has an important peak similar to the one in 4.1(c), and interestingly enough, there is a valley around $m_{PDG}(B)$. The signal of interest would be buried there. The corresponding filtered plot 4.1(f) contains 16602 events, where 2005 of them are within the mass window.

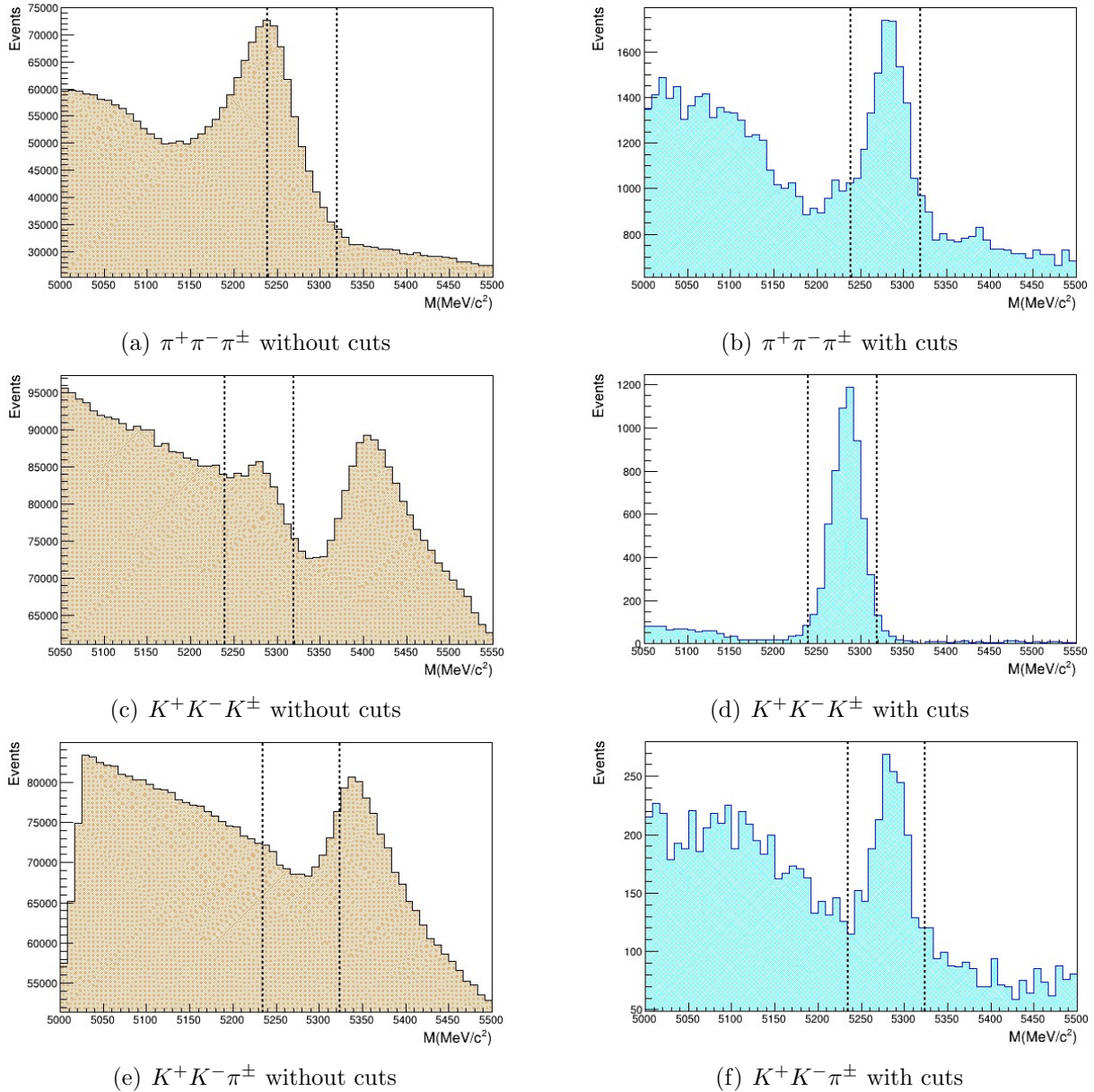


Figure 4-1.: Reconstructed mass of the initial state in the three decay systems using different sets of data

It is fair to assume that not much information can be obtained from the raw plots before cuts at first glance, because these come from using the final state particles of all events arbitrarily as the desired kaons and pions of the studied systems. However, it is interesting to note how the number of events composing the distributions within the mass window actually accounts for the data behavior around the B^\pm literature mass in the raw plots, whether or not there is a peak around $m_{PDG}(B)$ and how prominent it can be. More explicitly, the mass window with the highest filtered histogram event number (13091) is that coming from a raw histogram with an important peak near $m_{PDG}(B)$, while the mass window with the lowest filtered histogram event number (2005) is that with a corresponding raw histogram where nothing can be spotted around $m_{PDG}(B)$.

With normalized plots put together, it is possible to compare the shapes of the histograms before and after the cuts for all three systems on Figure 4-2. The plots also contain a vertical dotted line in orange representing $m_{PDG}(B)$.

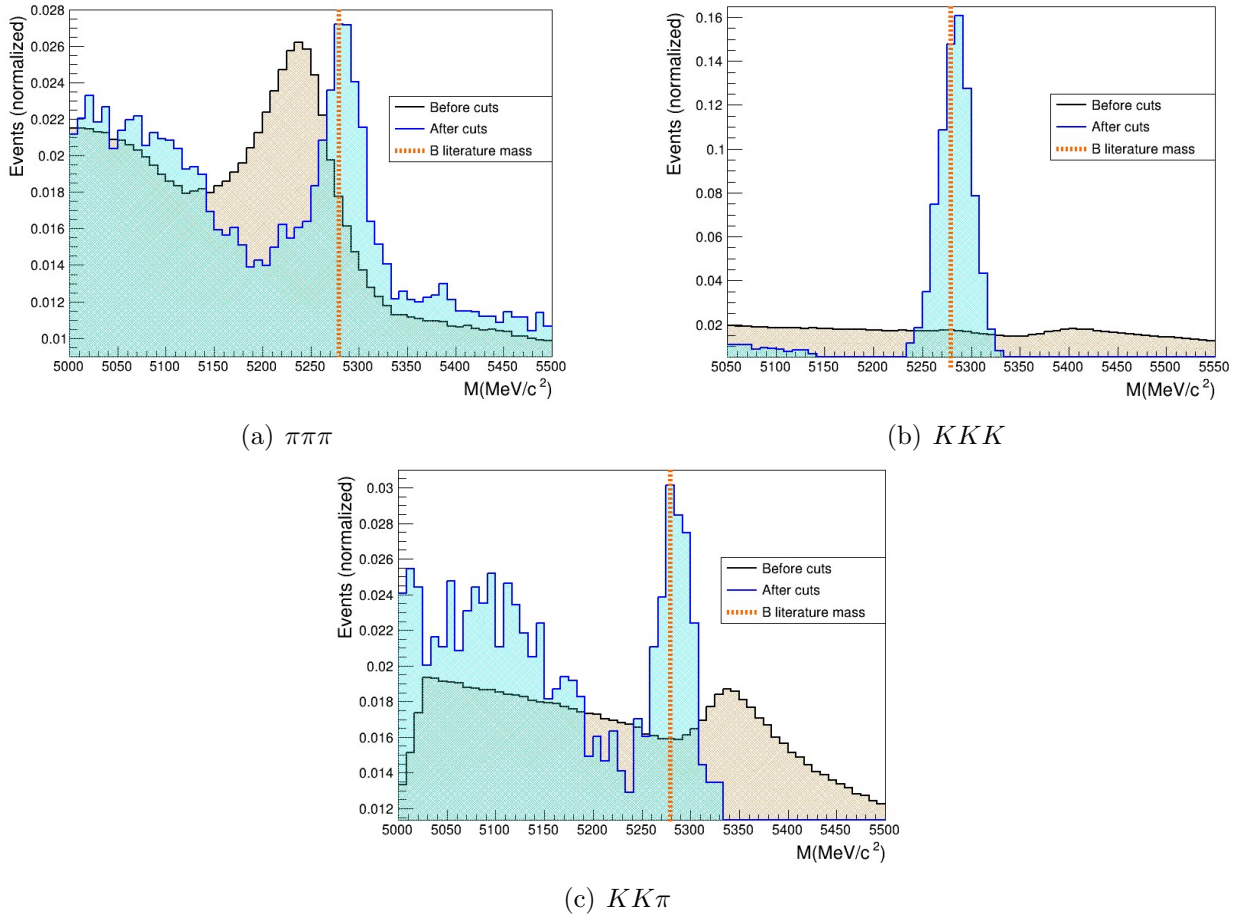


Figure 4-2.: Superposition of normalized raw and filtered plots for the reconstructed mass of the initial state in the three decay systems

Events of the filtered histograms in all cases are evidently distributed around $m_{PDG}(B)$, their peaks are very close if not onto it. These distributions around the mass of the object of interest are the signal, and it can be seen that the filtered histograms preserve a remainder of the background events that could be more or less important depending on the case. The cleanest filtered histogram, i.e. the one closest to containing only the signal, is the one for the KKK system. Signal histograms are commonly modeled by gaussian or Breit-Wigner distributions.

4.2. Adaptive binning of the Dalitz plots

Looking for an ideal visualization of the resonances in the phase space, which refers to the hadronic dynamics of intermediate states in the decay, an adaptive binning is worked out for the Dalitz plots. This means that the two-dimensional bins will not have the same size in general, but rather different widths and heights defined by the amount of events that would fall into their inner delimited area of the phase space.

While any binning structure would work, an adaptive treatment is much better to delimit the regions of interest and then be able to spot the differences in the number of events coming from B^+ and B^- in said regions. Figure 4-3 illustrates the situation, being the result of filling the phase space with all the objects of interest in the $\pi\pi\pi$ system, that is, using all the events filtered after applying the entire set of data cuts except for the one that separates the events by their net charge.

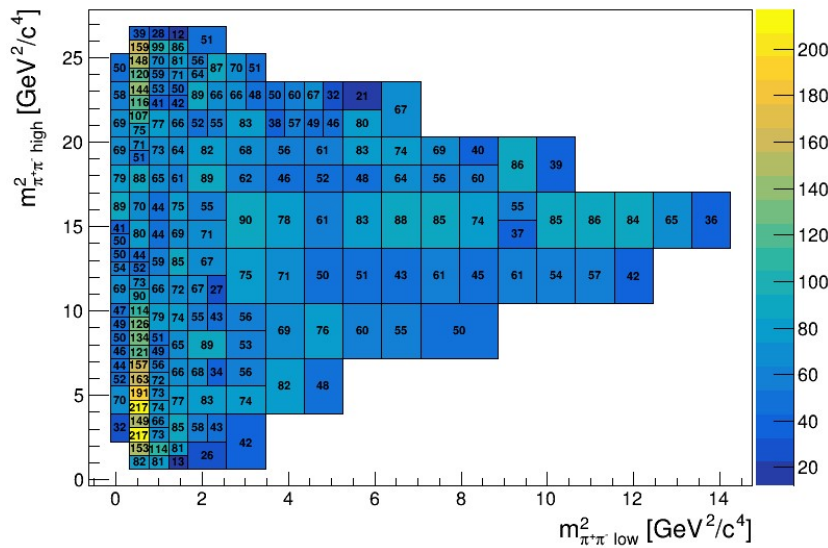


Figure 4-3.: Dalitz plot of event number, containing $m^2_{\pi^+\pi^-\text{low}}$ and $m^2_{\pi^+\pi^-\text{high}}$ variables of both B^+ and B^- candidates in the $\pi\pi\pi$ system

A binned Dalitz plot is directly a heat map, where in this case its color z -axis accounts for the number of events inside each bin. The idea is to localize the regions where most events fall in, which are where the resonances show up and become evident on the phase space. It can be seen that said regions are near the left border of the plot, parallel to the $m_{\pi^+\pi^-}^2$ axis. The rest of the plot shows a rather uniform distribution of events that would normally come from the remaining background of the filtered data, it is the blue-scale region covering the majority of the area.

Once the adaptive binning is created with filtered events of a given decay system, the resulting binning structure is applied to the two Dalitz plots that will later be filled out separately with the system's B^+ and B^- candidates. The same procedure is made to each of the three decay systems in the present work. Asymmetry calculations will simply operate the number of events from both plots of a given system according to equation 3-2. The adaptive binning consists of an algorithm that starts by considering the entire phase space as a single bin, then vertical and horizontal divisions take place based on the count of events inside the bins after each iteration. There is a count threshold, under which no more divisions would take place. Two parameters are to be controlled then, the number of iterations and the count threshold. It is important to note that both parameters, but especially the count threshold, have incidence over some of the later asymmetry calculations.

4.3. Study of the asymmetry

As mentioned in section 3.3, formal experimental results of CP asymmetry A_{CP} require a level of sophistication beyond the raw approximation in the present work, more specifically

$$A_{CP} = A_{raw} - A_D(\pi^\pm) - A_P(B^\pm) \quad (4-1)$$

where A_D is the pion detection asymmetry, associated with the possibility that the detector is more efficient in collecting pions of a given charge than the other, and A_P is the production detection asymmetry, associated with the possible production difference of B^+ and B^- coming out of the pp collisions. Those asymmetries are measured in experiments involving other decay channels, and would correspond to systematic uncertainties that must be considered in formal results of the channels of interest in this work.

It is intended to reproduce, at a raw-level of asymmetry, some of the results published in 2013 by CERN researchers [4][11]. **Local** and **global** raw asymmetry results are presented in this section, where local asymmetries refer to values coming out of calculations between B^+ and B^- bin level entries, while global asymmetries refer to values coming out of calculations between phase space level entries. Global results are independent of the adaptive binning, while local ones may depend on the binning structure.

4.3.1. $B^\pm \rightarrow K^+ K^- \pi^\pm$

The asymmetry plot of Figure 4-4 comes from a total number of 2005 events which passed through the cuts set for this system, falling into the $\pm 45 \text{ MeV}/c^2$ mass window around $m_{PDG}(B)$. The global asymmetry value is $-0,065 \pm 0,022$ (2.899σ), with maximum local $0.444 \pm 0,211(2,105\sigma)$ and minimum local $-0,727 \pm 0,146$ (4.970σ).

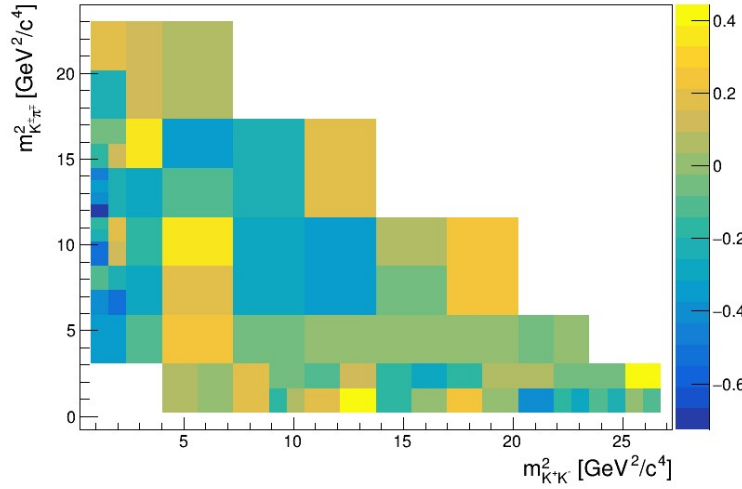


Figure 4-4.: Asymmetry of the number of events in binned Dalitz plot

The following histogram contains 1386 events from both B^+ and B^- decays, 238 from the region $m_{K^+K^-}^2 < 1,5 \text{ GeV}^2/c^4$ (showing the largest asymmetry) were used to calculate its local asymmetry as $-0,412 \pm 0,059$ (6.971σ)

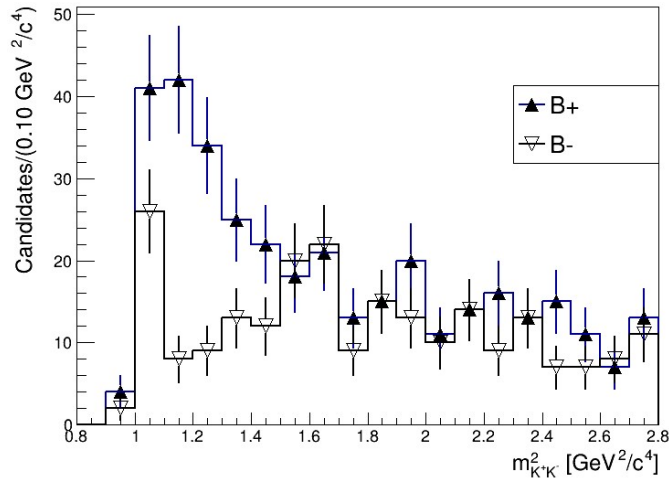


Figure 4-5.: Number of events in bins of the $m_{K^+K^-}^2$ variable

4.3.2. $B^\pm \rightarrow \pi^+\pi^-\pi^\pm$

The asymmetry plot of Figure 4-6 comes from a total number of 13091 events which passed through the cuts set for this system, falling into the $\pm 40 \text{ MeV}/c^2$ mass window around $m_{PDG}(B)$. The global asymmetry value is $0,045 \pm 0,009$ (5.103σ), with maximum local $0.446 \pm 0,111(4,019\sigma)$ and minimum local $-0,299 \pm 0,109$ (2.746σ).

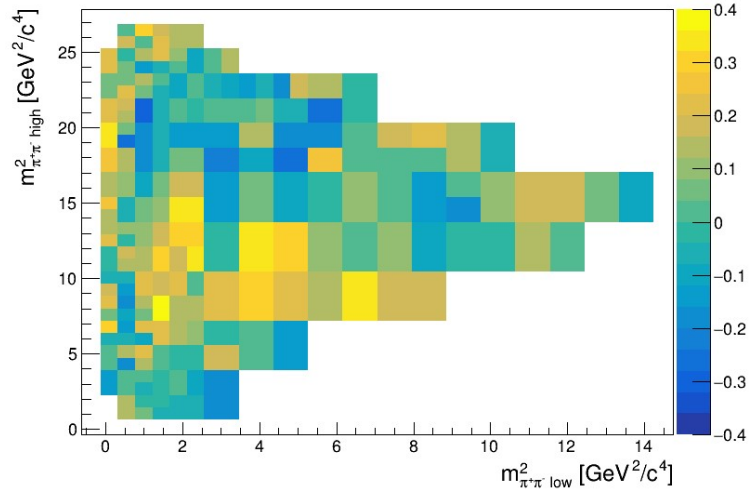


Figure 4-6.: Asymmetry of the number of events in binned Dalitz plot

The following histogram contains 6160 events from both B^+ and B^- decays, 571 from the region $m^2_{\pi^+\pi^- low} < 0,5 \text{ GeV}^2/c^4$ (showing the largest asymmetry) were used to calculate its local asymmetry as $0.243 \pm 0,040(5,997\sigma)$

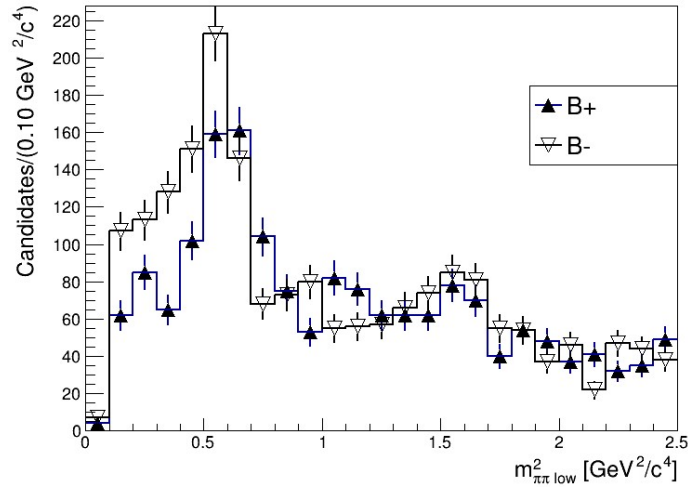


Figure 4-7.: Number of events in bins of the $m^2_{\pi^+\pi^- low}$ variable for $m^2_{\pi^+\pi^- high} > 15 \text{ GeV}^2/c^4$

4.3.3. $B^\pm \rightarrow K^+ K^- K^\pm$

The asymmetry plot of Figure 4-8 comes from a total number of 5954 events which passed through the cuts set for this system, falling into the $\pm 40 \text{ MeV}/c^2$ mass window around $m_{PDG}(B)$. The global asymmetry value is $-0,057 \pm 0,018$ (3.152σ), with maximum local $0.636 \pm 0,232$ ($2,736\sigma$) and minimum local $-0,778 \pm 0,210$ (3.712σ).

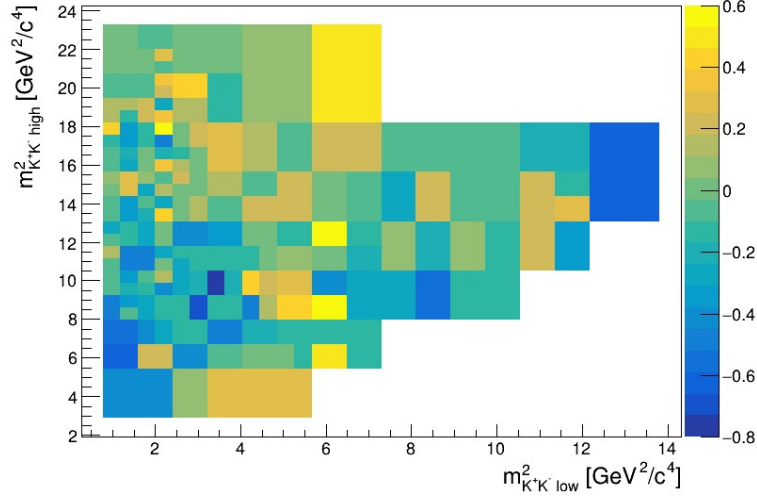


Figure 4-8.: Asymmetry of the number of events in binned Dalitz plot

The following histogram contains 3893 events from both B^+ and B^- decays, all were used to calculate its local asymmetry as $-0,096 \pm 0,016$ (6.038σ)

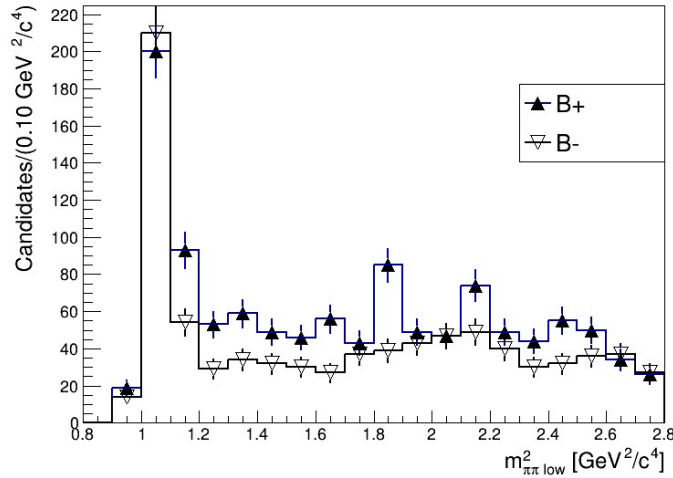


Figure 4-9.: Number of events in bins of $m_{K^+ K^-}^2$ variable for $m_{K^+ K^-}^2 < 15 \text{ GeV}^2/c^4$

5. Conclusions

CP violating effects were found in the studied systems. More specifically, based on the definition of significance for results, evidence and observations of direct CP violation were obtained in the phase space analysis of charged B meson decays. The presented uncertainties are purely statistical, lower significance is expected if processes involving systematic uncertainties are considered.

The global raw asymmetry results obtained for the $K^+K^-\pi^\pm$ and $K^+K^-K^\pm$ systems are compatible with the formal ones published in 2013, especially the one of the three K mesons. On the other hand, the raw asymmetry obtained for the $\pi^+\pi^-\pi^\pm$ system is outside of the formal result range.

The global raw asymmetry results obtained $A_{CP}(B^\pm \rightarrow K^+K^-\pi^\pm) = -0,065 \pm 0,022$ (2.899σ) and $A_{CP}(B^\pm \rightarrow K^+K^-K^\pm) = -0,057 \pm 0,018$ (3.152σ) are compatible with the formal results published in 2013, especially the one of the three K mesons. On the other hand, the result $A_{CP}(B^\pm \rightarrow \pi^+\pi^-\pi^\pm) = 0,045 \pm 0,009$ (5.103σ) is outside of the formal result range. This last fact can be attributed to the importance of the systematic uncertainties related to the pion detection asymmetry $A_D(\pi^\pm)$, since it's a three-pion final state system.

Accounting for well defined particle identification and selection criteria, results of 1-D histograms showing the largest asymmetry regions in all three systems are very similar to the ones in the reference articles published by CERN researchers in 2013. Asymmetry Dalitz plot results also allow a fairly good visualization of the regions of interest in all cases.

To count with a good event number for the analysis of the $KK\pi$ decay, wider ranges for hadron selection probabilities and mass window around $m_{PDG}(B)$ were necessary, since the event density in the phase space was not as large as in the other two systems. An important contributing factor is the symmetrization process that the other systems went through, due to having equal two-body invariant masses on each axis of the phase space.

Comparing the local results of the regions with larger asymmetry shown in the 1-D histograms of the three systems, the $B^\pm \rightarrow K^+K^-K^\pm$ one has the highest event number. That makes its raw local asymmetry the most solid result of all three, with a significance of over 6σ .

A. Attachment: Table of particles

Information on the mesons involved in this work is presented, mostly to show the mass values used in the calculations.

Meson	Quark composition	Mass (MeV/c ²)	Reference
B^+	$u\bar{b}$	5279.25 ± 0.17	[10]
K^+	$u\bar{s}$	493.677 ± 0.013	[12]
π^+	$u\bar{d}$	139.57039 ± 0.00018	[12]
D^0	$c\bar{u}$	1864.83 ± 0.05	[13]

Bibliography

- [1] HARRISON, Theresa: CP violation's early days. In: *CERN Courier* (2014), July
- [2] SUTTON, Christine: Fifty years of CP violation. In: *CERN News* (2014), August
- [3] BOUTIGNY, D. [u. a.]: *The BABAR physics book: Physics at an asymmetric B factory*. 1998
- [4] AAIJ, Roel [u. a.]: Measurement of CP violation in the phase space of $B^\pm \rightarrow K^+ K^- \pi^\pm$ and $B^\pm \rightarrow \pi^+ \pi^- \pi^\pm$ decays. In: *Phys. Rev. Lett.* 112 (2014), Nr. 1, p. 011801
- [5] YOUNG, Grace: New Package for RooFit Supporting Dalitz Analysis: RooAmplitudes. (2011), 01
- [6] GROUP, Particle D. ; ET AL., Zyla: Review of Particle Physics. In: *Progress of Theoretical and Experimental Physics* 2020 (2020), 08, Nr. 8. – 083C01. – ISSN 2050–3911
- [7] THOMSON, Mark: *Modern particle physics*. New York : Cambridge University Press, 2013. – ISBN 978–1–107–03426–6
- [8] BIGI, I. I. ; SANDA, A. I.: *CP Violation*. 2. Cambridge University Press, 2009
- [9] LHCb collaboration. Matter Antimatter Differences (B meson decays to three hadrons) - Project Notebook. CERN Open Data Portal. (2017)
- [10] ET AL., J. B.: Review of Particle Physics. In: *Phys. Rev. D* 86 (2012), Jul, p. 010001
- [11] AAIJ, R [u. a.]: Measurement of CP violation in the phase space of $B^\pm \rightarrow K^\pm \pi^+ \pi^-$ and $B^\pm \rightarrow K^\pm K^+ K^-$ decays. In: *Phys. Rev. Lett.* 111 (2013), p. 101801
- [12] ZYLA, P. A. [u. a.]: Review of Particle Physics. In: *PTEP* 2020 (2020), Nr. 8, p. 083C01
- [13] PATRIGNANI, C. [u. a.]: Review of Particle Physics. In: *Chin. Phys. C* 40 (2016), Nr. 10, p. 100001